arXiv:cond-mat/0509210v1 [cond-mat.str-el] 8 Sep 2005

Hidden magnetic order in the pseudogap phase of high-T_C superconductors

B. Fauque[1], Y. Sidis[1], V. Hinkov[2], S. Pailhes[1,3], C.T. Lin[2], X. Chaud[4] and P. Bourges[1]*

[1] Laboratoire Leon Brillouin, CEA-CNRS, CEA-Saclay, 91191 Gif sur Yvette, France

[2] MPI fur Festkorperforschung, Heisenbergstr. 1, 70569 Stuttgart, Germany

[3] LNS, ETH Zurich and Paul Scherrer Institute, CH-5232 Villigen PSI, Switzerland

[4] CRETA / CNRS, 25 Avenue des Martyrs, BP 166 38042 Grenoble cedex 9, France.

*To whom correspondence should be addressed; E-mail: bourges@llb.saclay.cea.fr

Abstract

One of the leading issue in high-T_C superconductors is the origin of the pseudogap phase in underdoped cuprates. Using polarized elastic neutron diffraction, we identify a novel magnetic order in the $YBa_2Cu_3O_{6+x}$ system. To date, it is the first direct evidence of an hidden order parameter characterizing the pseudogap phase in high-T_C cuprates. The observed magnetic order does not break the translational symmetry. It is basically consistent with the orbital moments expected in the circulating current theory of the pseudogap state.

All the high-temperature cuprate superconductors exhibit the same remarkable phase diagram. These compounds are antiferromagnetic (AF) insulators at zero doping and then become superconductors with hole doping; the superconducting (SC) transition temperature T_c exhibits a dome-like shape and reaches a maximum for an optimal doping, n_{opt}. In the underdoped state, defined by the doping levels lower than n_{opt}, the copper oxide superconductors display an unconventional metallic state [1, 2, 3, 4] with anomalous magnetic[5], transport[6], thermodynamic[7] and optical[3] properties below a temperature, T^*, larger

than T_c. All these intriguing properties point towards the opening of a pseudogap at the Fermi level [2, 3, 4] below T^*, whose spectroscopic evidences [2, 4] came from the leading-edge gap measured in angle-resolved photoemission (ARPES) experiments as well as from scanning tunneling microscopy, electronic Raman spectroscopy and optical conductivity [3].

A leading issue in high-T_C superconductors is the origin of that pseudogap phase [1] as its understanding should eventually lead to identify the superconducting mechanism. Two major classes of theoretical models attempt to describe the pseudogap state: in a first case, it represents a precursor of the superconducting d-wave gap [8, 9] with preformed pairs below T^* which would acquire phase coherence below T_c [9, 10]. In a second approach, the pseudogap is associated either with an hidden order [11, 12, 13, 14, 15, 16] or with a disordered phase [1, 17, 18] competing with the SC one and which opens a gap in the single-particle excitation spectrum. In such a case, the phase diagram versus doping is governed by a quantum critical point (QCP) below which the hypothetical order parameter is non-zero. The order parameter may involve charge and spin density waves [14, 15, 16] or charge currents flowing around the CuO_2 square lattice (flux phase) [11, 12, 13] as sketched in Fig. 1.a-c. In the latter case, one may have a single charge current per CuO_2 plaquette staggered in the neighboring cell, D-density wave (ddw) phase [13] (Fig. 1.a), or 4 (phase $_I$, Fig. 1.b) or 2 (phase $_{II}$, Fig. 1.c) current loops per unit cell, orbital circulating currents (CC) phases [11, 12]. The first case breaks the translational symmetry of the crystal whereas the two others preserve it as the loops are staggered within each unit cell.

Interestingly, these charge currents phases can be uniquely identified by virtue of the pattern of ordered orbital magnetic moments pointing perpendicularly to the CuO_2 planes (see Fig. 1). These orbital magnetic moments should be detectable by neutron diffraction. Although the hidden order scenarios are very appealing, they are not so far supported by many experiments. On the one hand, the absence of systematic staggered magnetic peaks at Q = (1/2,1/2) (;) in neutron scattering experiments for a given doping [19, 20, 21] makes the D-density wave scenario [13] unlikely. The CC state, as proposed at first by C.M. Varma [11] (phase $_I$), has not been detected by polarized elastic neutron experiments [22, 23]. On the other hand, recent ARPES measurements using circularly polarized photons in the $Bi_2Sr_2CaCu_2O_{8+}$ system [24] show a dichroic signal at the wavevector M = (,0) where the

pseudogap is maximum which indicates a time reversal breaking symmetry in the pseudogap state[24]. Among the CC phases [11, 12], the hidden order parameter proposed to describe the ARPES dichroism is compatible only with the CC phase having 2 current loops per CuO_2 unit cell (phase $_{II}$) [12].

We have performed polarized elastic neutron scattering experiments to test the orbital moments of this CC state, phase $_{II}$, which actually had never been attempted before. As a matter of fact, Bragg magnetic peaks characteristic (see Fig. 1) of the two CC states proposed by Simon and Varma[12] typically differ by 45 : main Bragg peaks like Q = (1 1 L) are expected for the state $_{I}$ and like Q = (1 0 L) [(0 1 L)] for the state $_{II}$. The previous unsuccessful polarized neutron diffraction experiments[22, 23] have focused on Bragg peaks along the diagonal direction, like Q = (1 1 L), characteristic of CC phase with 4 current loops per unit cell[11, 12]. We report the first signature of a novel hidden magnetic order in the $YBa_2Cu_3O_{6+x}$ (YBCO) system in the pseudogap phase in high-T_C cuprates. The magnetic scattering is basically consistent with the moments expected in the circulating current theory of the pseudogap state[11], specifically with the CC phase with two current loops per CuO_2 unit-cell [12].

All the polarized neutron diffraction measurements were collected on the 4F1 triple-axis spectrometer at the Laboratoire Leon Brillouin (LLB), Saclay (France). Our polarized neutron diffraction setup is similar to that originally described in [25] with a polarized incident neutron with at $E_i = 14.7$ meV obtained with a polarizing mirror (bender) and with an Heusler analyser (see also ref. [19, 22] in the context of high-T_C cuprates). The direction of the neutron spin polarization, P, at the sample position is selected by a small guide field H of the order of 10 G. Using that configuration, we then monitor at each measured point the neutron scattering intensity in the spin-flip (SF) channel, where the magnetic intensity, / M^2 (M is the magnetic moment), is expected, and the non-spin-flip (NSF) channel measuring the nuclear Bragg scattering. To have similar counting statistics on both SF and NSF, we count the SF channel systematically 20 times longer than the NSF. We define the normalized spin-flip intensity as $I_{norm} = I_{SF}/I_{NSF}$ (inverse of the flipping ratio (FR)). With that setup, a typical flipping ratio, ranging between 40 and 60, is easily realized. However, even with that high FR, the SF intensity is massively coming from the NSF nuclear

Bragg peak through unavoidable polarization leakage (corresponding to about 90-95% of the SF intensity). As a very stable FR is essential through the data acquisition, all the data have been obtained in a continuous run versus temperature. We prove that method to be efficient enough to see weak magnetic moments (0.05 $_B$) on top of nuclear Bragg peaks, see e.g. the first determination of the A-type antiferromagnetism in Na cobaltate systems[26].

We quote the scattering wave vector as Q = (H,K,L) in units of the reciprocal lattice vectors, a b = 1.63 A ^{1} and c = 0.53 A ^{1}. Most of the data have been obtained in a scattering plane where all Bragg peaks like Q = (0,K,L) were accessible (in twinned samples, this is indistinguishable from Bragg peaks with Q = (H,0,L)). In order to evidence small magnetic moments, measurements have been performed on the weakest nuclear Bragg peaks having the proper symmetry for the CC phase (the Bragg point Q = (0,1,1) offers the best compromise).

We have studied 5 different samples (see Table 1): 4 samples in the underdoped regime and one in the overdoped regime. In Fig. 2.a, we report the raw neutron intensity measured at Q = (011) for the spin flip (SF) channel and for the non-spin-flip (NSF) channel for an underdoped sample $YBa_2Cu_3O_{6.6}$ (d) (sample C). It has been obtained for a neutron polarization P//Q (see Fig. 2.b) where the magnetic scattering is entirely spin-flip because neutron diffraction measures only magnetic components perpendicular to the scattering wavevector[25, 22, 19]. Between room temperature and a temperature T_{mag}' 220K, the NSF and SF intensities display the same evolution, then, for $T < T_{mag}$, the NSF is essentially flat whereas the SF intensity increases noticeably at low temperature. This behaviour signals the presence of a spontaneous magnetic order below T_{mag} on top of the nuclear Bragg peaks. In Fig. 2.c, we represent the normalized magnetic intensity as a function of the temperature for the 4 underdoped samples and the overdoped sample. For the 4 underdoped samples, the magnetic intensity increases at low temperature below a certain temperature T_{mag} whereas no magnetic signal is observed in the Ca-YBCO overdoped sample (sample E). Using a simple fit of the evolution of the magnetic intensity with temperature (see Fig. 2 caption), one can deduce T_{mag} for each sample. T_{mag} decreases with increasing doping (see table 1) as expected from the pseudogap behaviour.

Therefore, we observe an unusual magnetic order in a temperature and doping range which fully covers the range where the pseudogap state is observed. The deduced T_{mag} matches the pseudogap temperature, T , of the resistivity data in YBCO [6] as shown on the Fig. 3. The occurrence of a magnetic order in this temperature and doping range then points towards a magnetic signature of an hidden order parameter associated with the pseudogap state. Being on top of nuclear Bragg peaks, that magnetic order does not break the translational symmetry of the lattice. Further, as shown in Fig. 2.c, no magnetic intensity occurs below T_{mag} at the Bragg peak $Q = (0;0;2)$ (as shown for samples A and C). This rules out regular ferromagnetism as the origin of the magnetic order. From our present measurements we cannot easily distinguish (without a detailed study of form factors) between scattering from spin or orbital moments. However, among the proposed order parameters, the only one which gives magnetic scattering at $Q = (10L)[(01L)]$ is the orbital moments arising from the circulating current phase with 2 current loops per CuO_2 unit cell, $_{II}$ [12] (Fig. 1.c). Note that the observation of a magnetic intensity at Q = (101) [(011)] rules out the $_{I}$ CC state where systematic extinctions occur for this phase (see Fig. 1.b). Further, additional unpolarized diraction neutron measurements at the AF wavevector, Q = (1/2,1/2), where magnetic Bragg peaks are expected for the D-density wave state (see Fig. 1.a), show no peak for the samples B, C and D (within our experimental limits $M_{AF} < 0:01\ _{B}$) whereas an in-plane magnetic ordering occurred at that AF wavevector in sample A, M_{AF} $0:05\ _{B}$ at 60 K [19].

We should stress that the observed magnetic order is characterized by 3D correlations with typical correlation lengths larger than 50 A. As shown in Fig. 2.c, the typical cross-section of the magnetic order is 1{2 mbarns, i.e. 10^{4} of the strongest Bragg peaks explaining why such a magnetic order was not reported before with regular unpolarized neutron diraction. Due to these experimental limitations, we do not perform a detailed and quantitative determination of magnetic structure for which further work is needed. However, some qualitative aspects can be briey discussed by looking at other Bragg peaks along c (or $Q = (0;1;L)$). First, we found that the magnetic intensity is not uniformly distributed versus L meaning that the magnetic intensity is not arising from the Cu-O chains. Second, from the hierachy of the observed magnetic intensities (intensity at L = 0 is larger than at

L = 2), the moments arrangement within a bilayer appears to be mainly parallel. Third, using the observed magnetic cross-section (Fig. 2.c) and a weakly momentum dependent form factor, one can deduce a typical magnitude of ordered magnetic moment of $M \simeq 0.05$ to $0.1\ _B$ with the moment decreasing with increasing doping in the 4 samples.

To determine the direction of these magnetic moments, we perfomed additionnal measurements where the neutron polarization was along the complementary directions, as shown in Fig. 2.b, either the vertical direction $P//z$, or the $P \perp Q$ but still within the horizontal scattering plane. The consistency of the amplitude of the low temperature signal in the three polarizations, as shown in Fig. 2.c, Fig. 2.d and Fig. 2.e for sample B, further proves its magnetic origin. In the $P//z$ configuration, only magnetic moments within the horizontal scattering plane but still perpendicular to Q are observed in SF channel [25, 22, 19]. For $Q = (0;1;1)$, this means that we mostly probe the magnetic moments parallel to the c axis. In the 4 underdoped samples, we observe a similar onset of the magnetic order below T_{mag} as for $P//Q$ (Fig. 2.d). This demonstrates that the deduced magnetic moment has a well-defined component perpendicular to the CuO_2 plane. However, a closer comparison of both polarizations reveals that their intensities do not simply match. More specifically, the magnetic moment is mostly along c for sample A (similar cross-section in Fig. 1.c and Fig. 1.d) but not for sample C (and in a lesser extent for sample B and D) where a non-negligible in-plane component (within the CuO_2 plane) needs to be invoked to explain the data (weaker cross-section in Fig. 1.d than Fig. 1.c).

Clearly, an in-plane magnetic component is not expected within the simple orbital moments picture discussed so far of currents flowing within perfectly flat CuO_2 planes. However, due to the dimpling of CuO_2 planes in YBCO, a weak in-plane moment can be produced as the effective moments at the centers of the O-Cu-O plaquettes are perpendicular to these plaquettes. Such an in-plane moment may be sufficient to describe the data in samples A, B and D but not for sample C. Within an orbital moment picture, spin degree of freedom might also play a role in producing in-plane magnetic moments, for instance, by spin-orbit coupling [27] or in relation to chiral spin states associated with flux phases [28]. Alternatively, this could imply that the observed magnetism might be due to electronic spins although no existing spin model gives the observed magnetic scattering.

In conclusion, we report a signature of an unusual magnetic order in several $YBa_2Cu_3O_{6+x}$ samples matching the pseudogap behaviour in underdoped cuprates (Fig. 3). Such an observation points towards the existence of an hidden order parameter for the pseudogap phase in high-T_C superconductors. Importantly, this order does not break the translational symmetry of the lattice. Despite an unexpected in-plane magnetic component, the symmetry of the observed order is consistent with the proposal of orbital moments emanating from a circulating currents state [11, 12].

Acknowledgements: We are very grateful to C.M. Varma for invaluable encouragement, critics and ideas on these experiments. We also thank B. Keimer, J.-M. Mignot, P. Monceau, L. Pintschovius, and L.-P. Regnault for their support.

References

[1] M.R. Norman, D.P. Pines, & C. Kallin, preprint cond-mat/0507031.

[2] M.R. Norman & C. Pepin, Rep. Prog. Phys. 66, 1547 (2003).

[3] T. Timusk, & B. Statt, Rep. Prog. Phys. 62, 61 (1999).

[4] J.L. Tallon & J.W. Loram, Physica C 349, 53 (2001).

[5] H. Alloul, T. Ohno, & P. Mendels, Phys. Rev. Lett. 63, 1700 (1989).

[6] T. Ito, K. Takenada, & S. Uchida, Phys. Rev. Lett. 70, 3995 (1993).

[7] J.W. Loram, et al. Physica C, 235-240 134 (1994).

[8] P.A. Lee, Physica C 317{318, 194{204, (1999).

[9] V.J. Emery & S.A. Kivelson, Nature 374, 434 (1995).

[10] J. Orenstein, & A.J. Millis, Science 288, 468 (2000).

[11] C.M. Varma, Phys. Rev. B, 55, 14554 (1997); Phys. Rev. Lett. 83, 3538 (1999); preprint, cond-mat/0507214.

[12] M. E. Simon & C. M. Varma, Phys. Rev. Lett. 89, 247003 (2002).

[13] S. Chakravarty, et al. Phys. Rev. B 63, 094503 (2001).

[14] C. Castellani, et al. Phys. Rev. Lett. 75, 4650 (1995).

[15] H. C. Chen, et al. Phys. Rev. Lett. 93, 187002 (2004).

[16] D. Poilblanc, cond-mat/0503249.

[17] J. Zaanen, et al. Phil. Mag. B, 81, 1485 (2001).

[18] F. Onufrieva, & P. Pfeuty, Phys. Rev. Lett., 82, 3136 (1999).

[19] Y. Sidis, et al. Phys. Rev. Lett. 86, 4100 (2001).

[20] H. A. Mook, et al. Phys. Rev. B 66, 144513 (2002).

[21] C. Stock, et al., Phys. Rev. B 66, 024505 (2002).

[22] S. H. Lee, et al. Phys. Rev. B 60, 10405 (1999).

[23] Ph. Bourges, L. P. Regnault, J. Y. Henry, & C. Marin, Unpublished data (1998).

[24] A. Kaminski, et al., Nature 416, 610 (2002).

[25] R. M. Moon, et al. Phys. Rev. 181, 920 (1969).

[26] S. P. Bayrackl, et al. Phys. Rev. Lett. 94, 157205 (2005).

[27] C. Wu, Y. Zaanen & S. C. Zhang, cond-mat/0505544.

[28] X. G. Wen, et al. Phys. Rev. B, 39, 11413 (1989).

[29] V. Hinkov, et al., Nature 430, 650 (2004).

[30] L. Pintschovius, et al., Phys. Rev. Lett. 89, 037001 (2002).

[31] J. L. Tallon, et al., Phys. Rev B, 51, 12911 (1995).

Table:

label	x	$T_{c,onset}$ (K)	T_{mag} (K)	References
A	$O_{6.5}$ (t)	un 54	300 10	[19]
B	$O_{6.6}$ (t)	un 61	250 20	[30]
C	$O_{6.6}$ (d)	un 64	220 20	[29]
D	$O_{6.75}$ (t)	un 78	170 30	–
E	Ca(15%) O_7 (t)	ov 75	' 0	–

Table 1: List of samples utilized in the polarized elastic neutron experiments. The experiments were performed in the (Y,Ca)$Ba_2Cu_3O_{6+x}$ family for 5 samples from the underdoped (un) to overdoped (ov) part of the cuprates phase diagram. (t) and (d) stands for twinned and detwinned samples, respectively. References are given where the samples have been described in previous neutron scattering studies. T_{mag} is the onset temperature of the novel magnetic order (see text).

Figure Captions:

Figure 1: Top panels sketch 3 different charge current phases in the CuO_2 plane proposed to explain the pseudogap phase in high-T_c superconducting cuprates. Low panels display, for each of these phases, the location of the Bragg spots in the planar (H,K) reciprocal space where magnetic scattering is expected in neutron diffraction experiments. The magnetic intensities are computed from the pattern shown in the top panels for a single CuO_2 plane per unit cell and taking into account of the different magnetic domains, but without considering the magnetic form factor of each current loop.

Figure 2: (a): Temperature dependencies of the raw SF and NSF neutron intensity measured at Q = (0,1,1) in sample C. (b) Sketch of the scattering plane showing the three polarization directions discussed here, P //z corresponds to the direction perpendicular to the scattering plane (here a). c) Temperature dependencies of the normalized magnetic intensity, I_{mag}, measured at Q = (0,1,1) for P //Q for the 4 underdoped samples (A,B,C,D) and the overdoped sample E (full points). I_{mag} is defined as $I_{mag}(T) = \frac{7}{I_{004}^{meas}(300K)} I_{NSF}(300K) [\frac{I_{SF}}{I_{NSF}}(T) - \frac{I_{SF}}{I_{NSF}}(T \quad 300K)]$ where (i) I_{mag} is arbitrarily set to zero in the high temperature range (room temperature), and (ii) the first term calibrates the magnetic intensity to the measured intensity of the nuclear peak Q = (004). I_{mag} is actually estimated in mbarns using the calculated nuclear Bragg cross-section of $I_{004}^{calc} = 7$ barns. The line corresponds to a fit using the functional form $I_{mag}(T) / (1 - (\frac{T}{T_{mag}}))$ for $T \quad T_{mag}$. The normalized magnetic intensity for the Bragg peak, Q = (0;0;2), is also shown for samples A and C (open points). d) Temperature dependencies of the normalized magnetic intensity, I_{mag}, measured at Q = (0,1,1) (full points) (as well as Q = (0,0,2), open points) for P //z. e) Temperature dependencies of the normalized magnetic intensity, I_{mag}, measured at Q = (0,1,1) for sample C for P ? Q.

Figure 3: Cuprate superconductors phase diagram as a function of hole doping, n_h, deduced from the SC temperature using the empirical relation $T_C/T_C^{max} = 1 \quad 82:6(n_h \quad 0:16)^2$ [31]. The white points show T_{mag} (see table 1). The color map shows the quantity $R(T) = \frac{1}{T}[\rho_{ab}(T) \quad \rho_{ab}(0)]$ deduced from the resistivity measurements in YBCO [6]: the change of colors indicates the departure from the T-linear behaviour, R(T) = 0 represented in blue, at high temperature. $R(T) \neq 0$ defines the pseudogap state.

Figure 1:

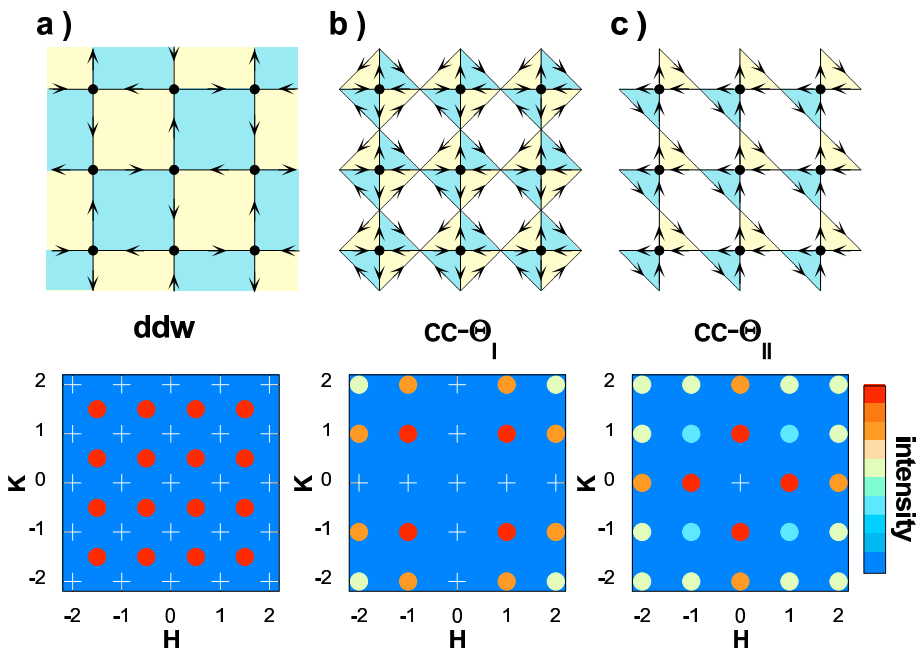

Figure 2:

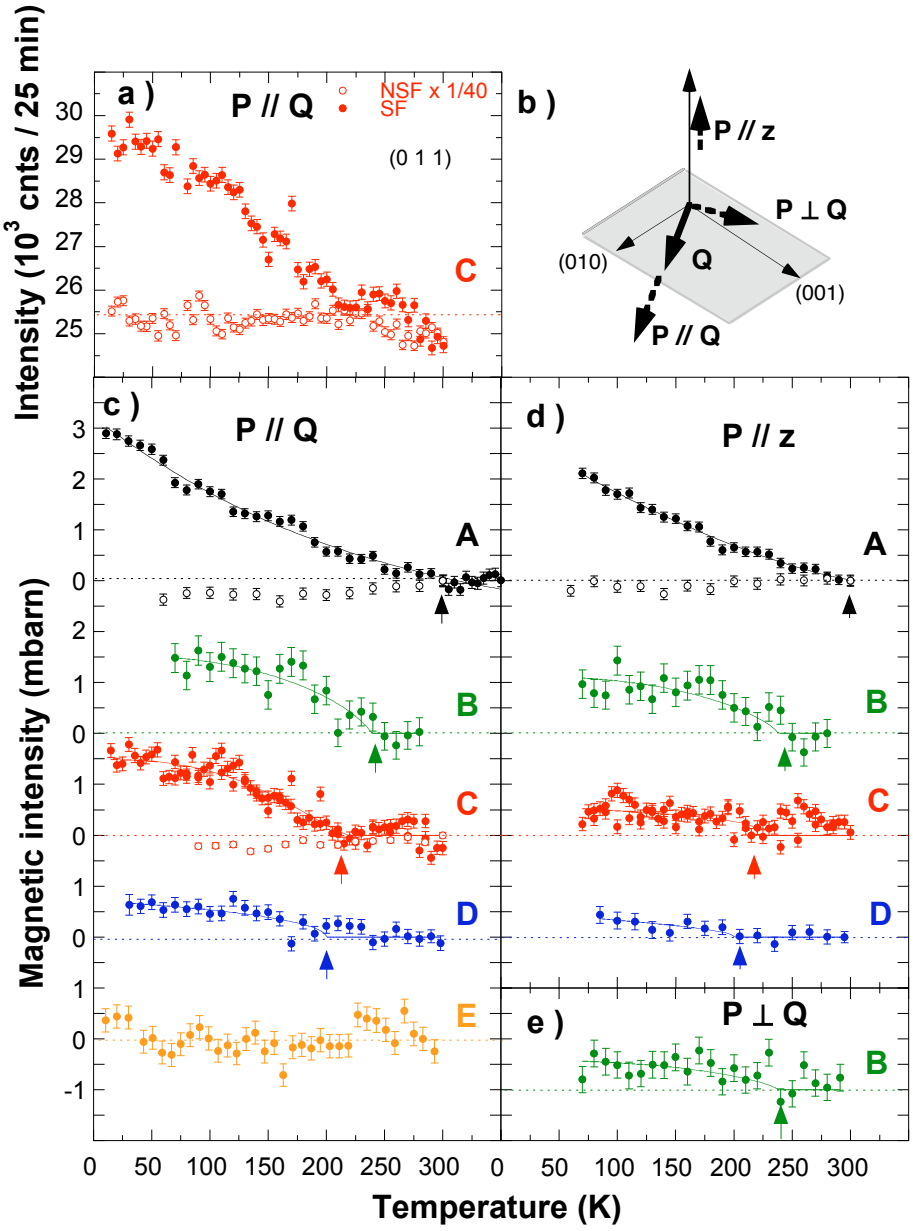
a)
P // Q
NSF x 1/40
SF
(0 1 1)
C
b)
P // z
P ⊥ Q
Q
(010)
(001)
P // Q
c)
P // Q
d)
P // z
A
B
C
D
E
e)
P ⊥ Q
B
Intensity (10^3 cnts / 25 min)
Magnetic intensity (mbarn)
Temperature (K)

Figure 3:

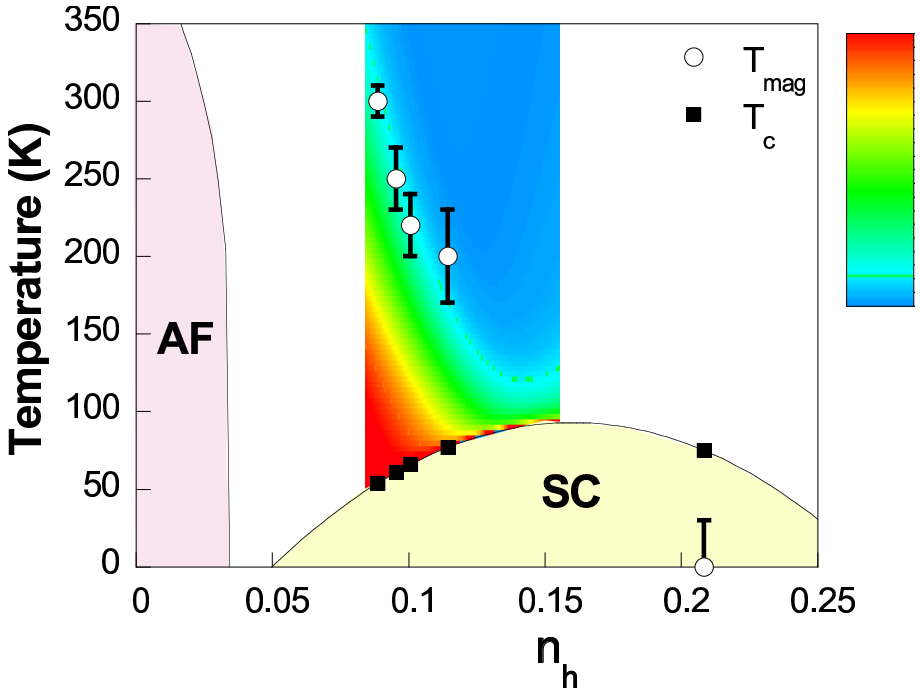
Temperature (K)
350
300
250
200
150
100
50
0
AF
SC
T mag
T c
0
0.05
0.1
0.15
0.2
0.25
n h